Supplementary material (ESI) for Journal of Materials Chemistry

Supplementary Materials

Surface Eu^{3+} ions are different than "bulk" Eu^{3+} ions in crystalline doped LaF_3 nanoparticles

V. Sudarsan and Frank C. J. M. van Veggel*

University of Victoria, Department of Chemistry, P. O. Box 3065, Victoria, British Columbia, Canada, V8W 3V6.

Rodney A. Herring

University of Victoria, Department of Mechanical Engineering, P. O. Box 3055, Victoria, British Columbia, Canada, V8W 3P6.

Mati Raudsepp

The University of British Columbia, Department of Earth and Ocean Sciences, Vancouver, British Columbia, Canada, V6T 1Z4.

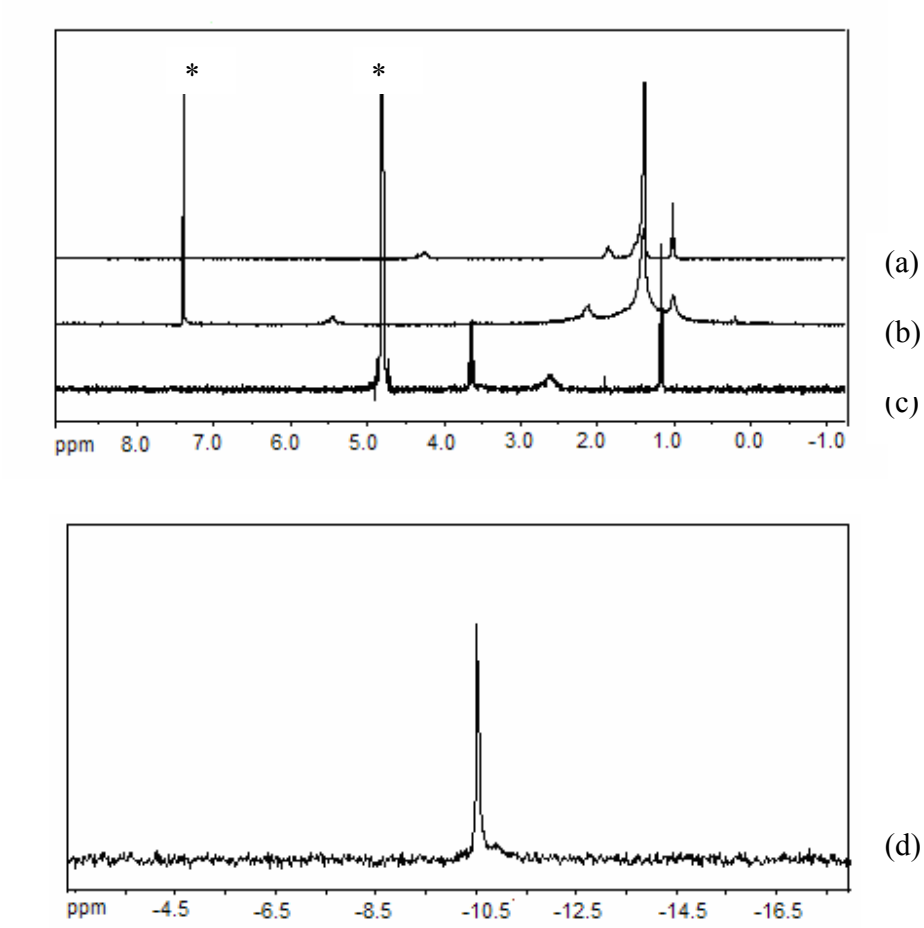

Figure S1, The ^{1}H NMR patterns for (a) LaF_3:Eu(5%) nanoparticles stabilised with di-n-octadecyl dithiophosphate ligand, (b) LaF_3:Eu(5%) nanoparticles stabilised with oleate ligand, (c) LaF_3:Eu(5%) nanoparticles stabilised with citrate ligand and (d) ^{31}P NMR pattern of LaF_3:Eu(5%) nanoparticles stabilised with polyphosphate ligand. The peaks marked " * " correspond to the solvents, $CDCl_3$ and water. The two sharp peaks observed ~3.6 ppm and 1.2 ppm in the citrate stabilised particles are arising from the residual ethanol left in the sample.

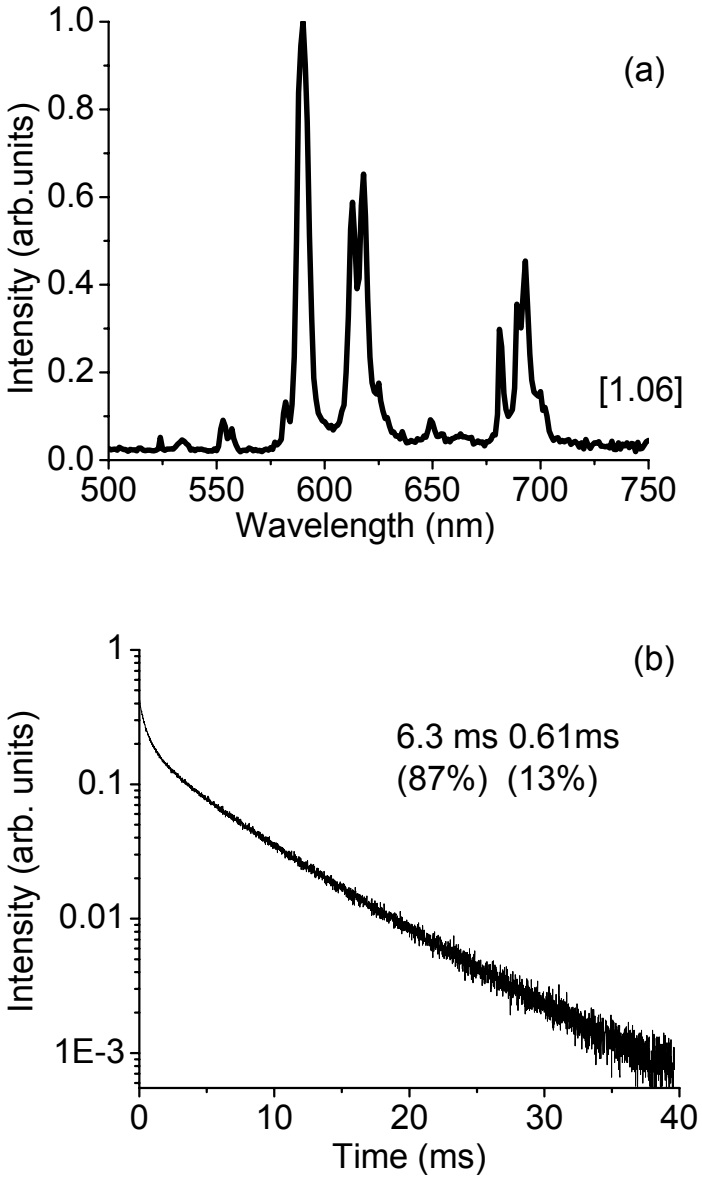

Figure S2, Emission spectrum (a) and the decay curve monitored at 590 nm (b) for LaF_3:Eu(2%) nanoparticles stabilised with di-n-octadecyldithiophosphate ligand. The asymmetric ratio is shown in square bracket.

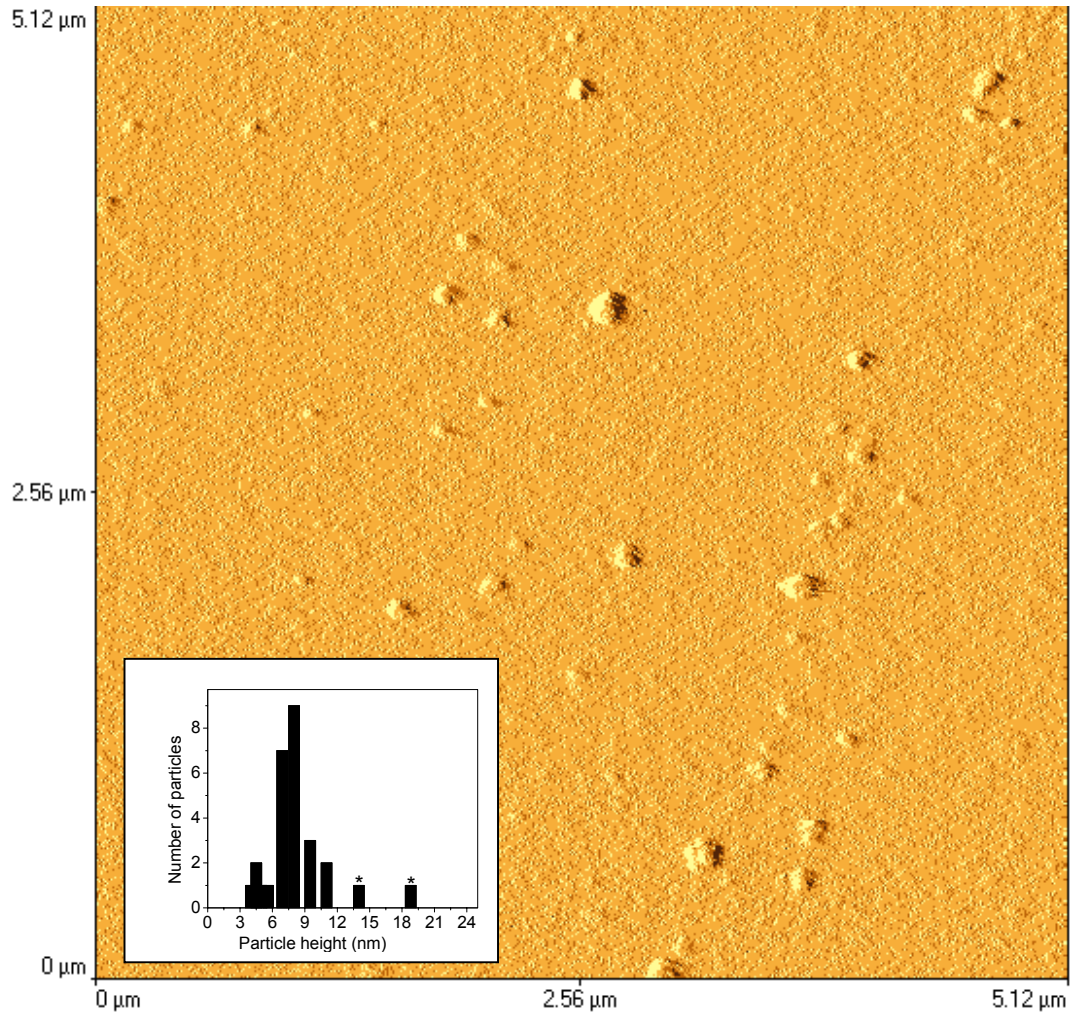

Figure S3, AFM image of LaF_3:Eu-LaF_3 core-shell nanoparticles stabilised with di-n-octadecyldithiophosphate ligand. The "*" marks in the histogram represent agglomerates.

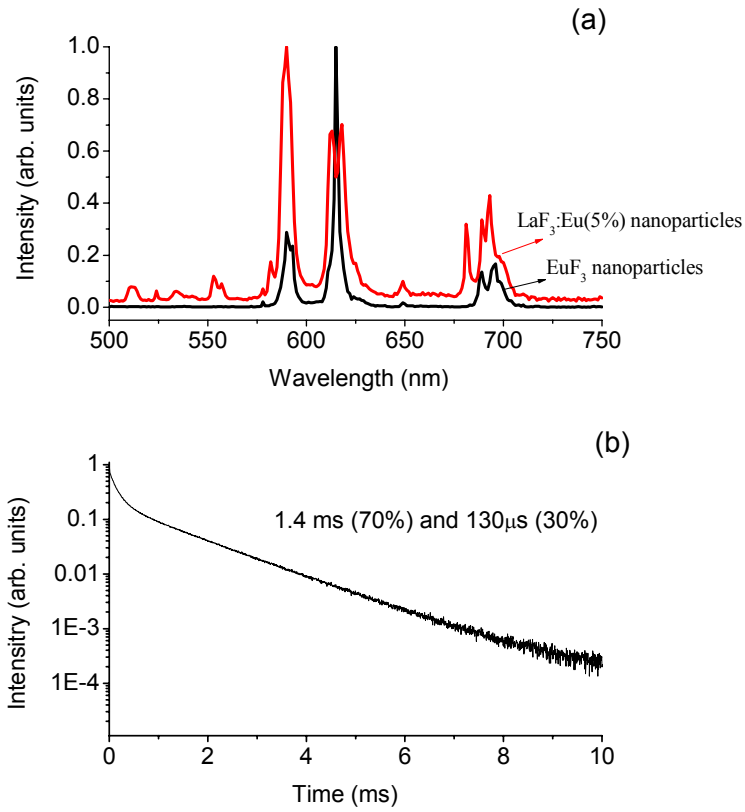

Figure S4, (a) Emission spectra corresponding to LaF_3:Eu nanoparticles (red) and EuF_3 nanoparticles (black). The decay curve corresponding to the 590 nm emission from EuF_3 nanoparticles are shown in Figure S4(b).The particles were stabilised with di-n-octadecyldithiophosphate ligand and excited at 397 nm for emission measurements and 464 nm for measuring the decay curve.

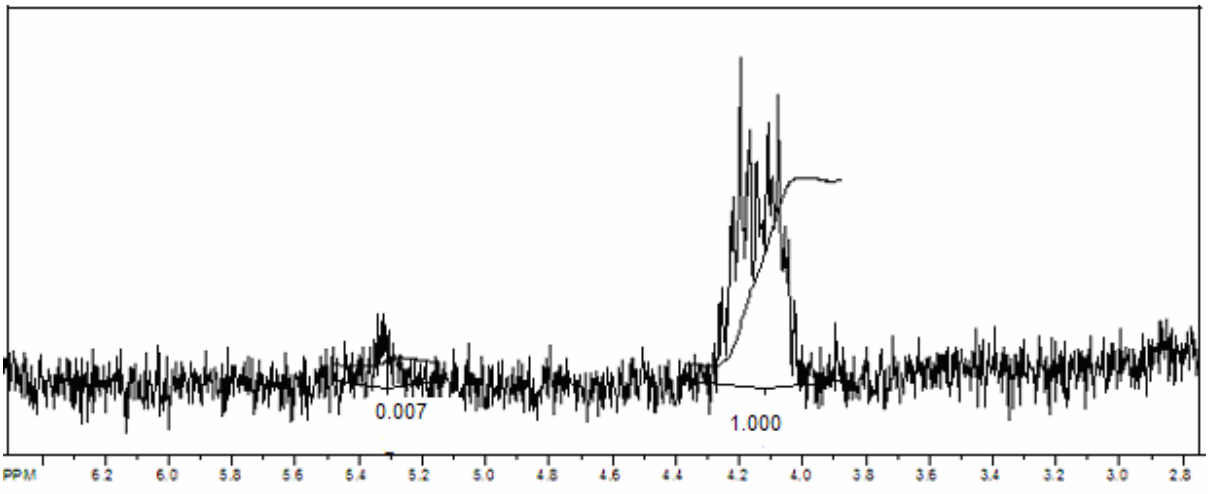

Figure S5, ^{1}H NMR pattern of a $CDCl_3$ solution containing 5 mg each of LaF_3:Eu(5%) nanoparticles, stabilised with di-n-octadecyldithiophosphate and oleate ligands. The peak at 5.1 ppm is characteristic of oleate ligand and that around 4.1 ppm is characteristic of di-n-octadecyldithiophosphate ligand.

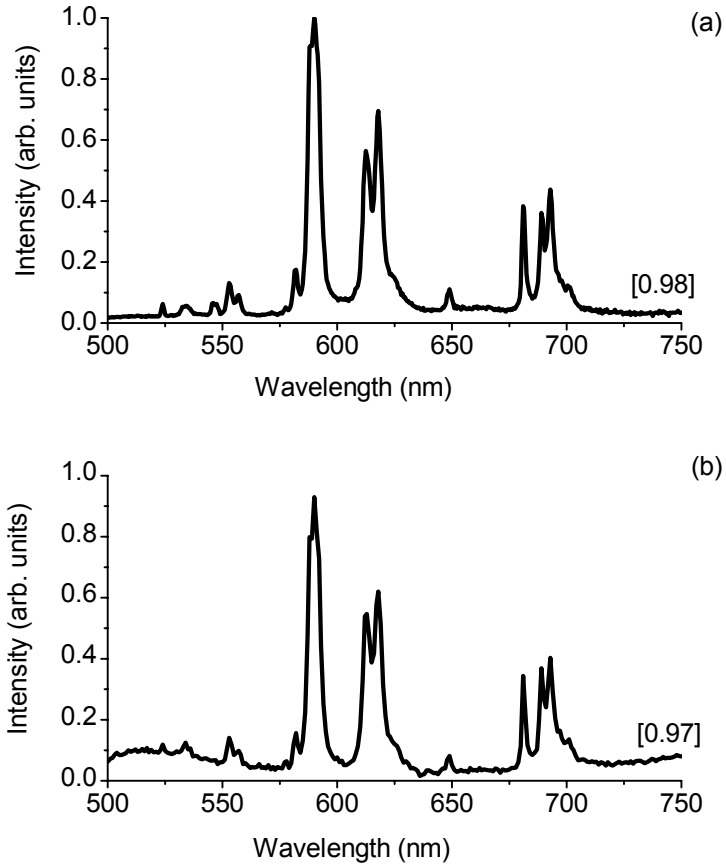

Figure S6, Emission spectra of LaF_3:Eu(5%)-LaF_3 core-shell particles stabilised with (a) di-n-octadecyldithiophosphate and (b) oleate ligands. The samples were excited at 397 nm. The numbers in square brackets show the asymmetric ratios.

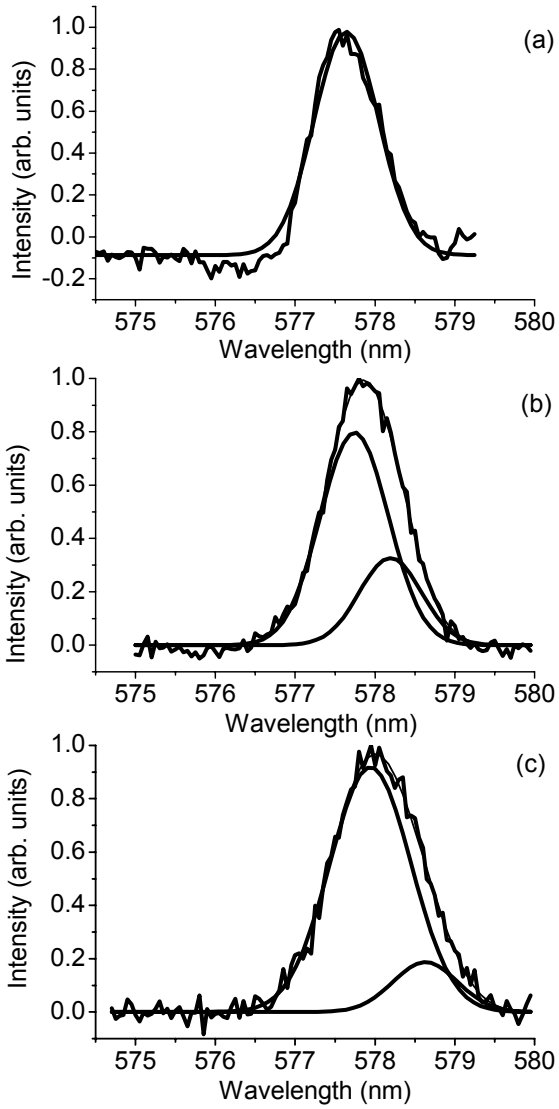

Figure S7, High resolution emission spectra corresponding to the $^5D_0 \rightarrow {}^7F_0$ transition for (a) LaF_3:Eu(5%)-LaF_3 core-shell nanoparticles stabilised with di-n-octadecyldithiophosphate ligand (b) LaF_3:Eu(10%) particles stabilised with oleate ligand (c) LaF_3:Eu(20%) particles stabilised with di-n-octadecyldithiophosphate ligand, recorded with a resolution of 0.1 nm. The samples were excited at 397 nm.

Supplementary material (ESI) for Journal of Materials Chemistry

Calculation of the $f_{q,i}$ values

The $f_{q,i}$ values are calculated by assuming that the quenching occurs via dipole-dipole mechanism and has a distance dependence of r^{-6}. Integrating this over the whole volume "v" out side the particles gives the total quenching factor $f_{q,i}$, for the i^{th} shell by the equation (1).[7]

$$f_{q,i}(a_i) = \int_{v} r^{-6} dV \qquad \text{.....(1)}$$

Where a_i is the centre of the i^{th} shell and can be represented as $a_i = A_i/R_i$. Since the particles are divided into "10" shells (n = 10), A_i values are same for all the shells ($A_i = 1/n = 0.1$). The A_i values mentioned here are different from the A_i values in the equation 5 of the manuscript. The value of R_i varies with shell radius "r". Schematic representation of a particle having a shell "*i*" with the symbols used in the text is given below.

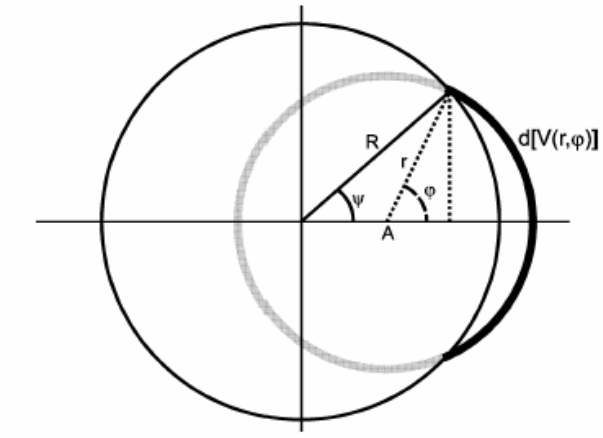

Figure S8. Schematic representation of a particle with the symbols used to calculate the $f_{q,i}$ values.

This equation was solved for each of the 10 shells by varying the a_i values. Brief description of the procedure used to solve the equation is given below.

The region around a Eu^{3+} ion in the particle can be divided in to three domains. The first domain is totally inside the particle with r = 0 to r = R-A, and hence there is no quenching from this domain. Second domain ranges from, r = R-A to R+A. In the second domain part of the shell is inside the particle and part is outside. The part which is outside the particle only contributes to quenching. The volume fraction d[V(r,φ)] outside the particle, depends on both the radius of the shell and the angle φ and can be expressed as $2\pi r^2(1-\cos\varphi)dr$. The third domain lies totally outside the particle and varies from r = R+A to ∞. The volume fraction the third domain can be expressed as $4\pi r^2 dr$. Hence combing these three domains, $f_{q,i}$ values can be expressed by the equation (2).

$$f_{q,i}(a_i) = \int_{v} r^{-6} dv = \int_{R-A}^{R+A} \frac{1}{r^6} 2\pi r^2 (1-\cos\varphi) dr + \int_{R+A}^{\infty} \frac{1}{r^6} 4\pi r^2 dr \qquad \text{.....(2)}$$

In the equation 2, 'ϕ' is a function of 'P', which in turn is a function of 'r'. The equation was numerically solved for all the 10 shells and the results are shown in Table S1. For core-shell particles, a similar procedure was used to calculate $f_{q,i}$ values, however the a_i values were recalculated considering the particle is made up of by 10 core shells surrounded by an undoped 11^{th} shell with same volume for all the shells. The values are shown in Table S1.

Supplementary material (ESI) for Journal of Materials Chemistry

Table S1. The values of "a_i" and "$f_{q,i}$" for both core and core-shell particles

Core nanoparticles			Core-shell nanoparticles	
Shell i	a_i	$f_{q,i}$	a_i	$f_{q,i}$
1	0.230	4.92	0.225	4.88
2	0.520	10.81	0.508	10.28
3	0.630	19.21	0.607	16.76
4	0.700	31.87	0.681	27.41
5	0.770	62.96	0.741	46.37
6	0.820	121.45	0.792	83.15
7	0.870	2.99×10^2	0.838	1.63×10^2
8	0.910	8.59×10^2	0.879	3.72×10^2
9	0.950	4.85×10^3	0.917	1.09×10^3
10	0.980	7.67×10^4	0.952	5.48×10^3